ISSN 1814-4225 (print)
ISSN 2663-2012 (online)

UDC 621.396

doi: 10.32620/reks.2025.2.10

Yasir M.Y. AMEEN, Marwan H. MOHAMMED, Basil M. SAIED

Department of Electrical Engineering, University of Mosul, Mosul, Iraq

EFFICIENT SYSTEM DESIGN OF CAPACITIVE COUPLING WIRELESS CHARGING FOR LOW-POWER APPLICATIONS

*The **subject matter** of this article is the design and analysis of charging pads based on capacitive coupling for wireless power transfer (WPT) in electric vehicle (EV) charging systems. **The main goal** of this study is to improve the efficiency and overall performance of CPT-based EV charging systems by enhancing the self-capacitance, increasing the coupling efficiency, and minimizing the reliance on oversized or auxiliary passive components while maintaining the compact pad geometry. To achieve this task, two novel four-sheet pad configurations are introduced and evaluated: The M2-four-sheet parallel formation, in which four aluminum sheets are arranged horizontally, and the M2-four-sheet stacked formation, in which the sheets are aligned vertically. Their performance was systematically compared with that of conventional four-sheet layouts to validate the proposed improvements. The proposed formations maintain equal pad dimensions (610 mm × 610 mm) on the primary and secondary sides to ensure effective coupling and high self-capacitance. **The methods** used include LCLC and LCL compensation topologies resonate with the capacitive coupler and deliver high voltage to the charging pads. Finite-element analysis (FEA) was employed to simulate the coupling capacitance and optimize the coupler's geometry, while MATLAB software was used to simulate the complete WPT system. **The results** show that the M2-four-sheet parallel formation achieved significantly higher self-capacitance compared to the traditional layout, with little variation in the coupling capacitance. The M2-four-sheet stacked formation provides even higher self-capacitance than the parallel one and enhances the overall system efficiency without increasing the pad size. Based on these findings, a 1.5-kW CPT system was designed using four aluminum pads with a 150-mm air gap, achieving a DC-DC efficiency greater than 90.5%. **Conclusions.** The M2-four-sheet parallel formation demonstrates a 175% increase in self-capacitance compared to the traditional layout. Meanwhile, the M2-four-sheet stacked formation improved the coupling coefficient by 21.4%, although it nearly half the self-capacitance relative to the traditional layout. Both designs contribute to significant improvements in system performance and efficiency. Therefore, this study presents a novel symmetric four-sheet pad configuration that significantly improves the self-capacitance and coupling performance, thereby reducing the reliance on external capacitors while maintaining compact geometry and high transfer efficiency.*

Keywords: *Wireless power transfer (WPT); Capacitive power transfer; electric vehicle charging; LCLC compensation; LCL compensation; four-sheet formation; capacitive coupler design.*

1. Introduction

Capacitive power transfer (CPT) is an efficient alternative to traditional inductive power transfer (IPT) and is widely used in wireless power transfer (WPT) [1-4]. CPT uses high-frequency electric fields, as opposed to the magnetic fields employed in IPT, for power transfer [5]. Magnetic fields can be affected by nearby metal objects, resulting in a rapid reduction in system efficiency when interference occurs [6]. These fields generate heat in conductive materials, leading to eddy current losses. Additionally, due to the skin effect in high-frequency conductors, the construction of coils requires a significant amount of Litz wire, which increases both the weight and cost of the system [1, 7]. The high-frequency electric fields used in CPT offer unique benefits, such as less eddy current loss, lightweight and inexpensive construction, superior misalignment performance, and the ability to avoid large losses in metal objects. As a result, CPT has grown rapidly in the WPT market [8, 9].

1.1. Motivation

Although CPT offers superior benefits, current CPT systems face challenges such as low self-capacitance and coupling efficiency, which often require oversized or additional components to achieve the desired performance. These limitations hinder the scalability and cost-effectiveness of wireless electric vehicle (EV) charging technologies, which are critical to meeting the growing demand for reliable and sustainable energy solutions in modern transportation systems. Addressing these issues is essential for advancing the field and enabling the widespread adoption of wireless charging technologies. Therefore, this study was motivated by the need to overcome these challenges by developing innovative charging pad designs that improve the performance of CPT systems.

1.2. State-of-the-Art

A typical formation of a CPT system is shown in Fig.1. It consists of rectifiers, a high-frequency inverter, compensation networks, and a capacitive coupler, enabling efficient AC-DC-AC conversion and transmission to the load. CPT is utilized in various applications, including EV charging applications [10], robotic joints [11], LED drivers [12], soccer robot charging [13], and synchronous motor excitation [14]. However, recent advancements in CPT systems have focused on optimizing coupler configurations and compensation topologies, whereas early CPT systems relied on simple two-sheet couplers [15] with basic LC compensation; however, their low coupling capacitance (in the nano-farad range) and rapid efficiency degradation at larger air gaps limited their practical adoption. To address these limitations, multi-sheet configurations have evolved: four-sheet parallel formations [9] improve the lateral misalignment tolerance (±15 cm) by maximizing the overlap area, while four-sheet stacked designs [16] enhance vertical coupling at extended air gaps (15–20 cm) through concentrated electric fields. Recent innovations, such as six-sheet underwater couplers [17], leverage water's high permittivity ($\varepsilon_r \approx 80$) to achieve 87.2% DC-DC efficiency over 60-mm gaps, although their complexity and environmental limitations hinder EV applicability in real life.

At the same time, compensation topologies have been developed to mitigate voltage stress and reactive losses. Double-sided LCL networks [18] eliminate parallel capacitors, achieving 90% efficiency with zero-phase-angle operation, while LCLC topologies [9] enable 90.8% efficiency at 2.4 kW but introduce complexity with eight external components. Despite progress, critical trade-offs persist in simplified LCL designs [16], sacrifice efficiency (85.87% at 1.88 kW) for fewer components, and high-frequency stabilization methods [19] (1.55 MHz) remain limited to low-power (25 W) applications. Furthermore, existing systems prioritize either lateral misalignment resilience (horizontal couplers) or air-gap tolerance (vertical stacks), neglecting dual-use versatility. This work bridges these gaps by proposing a symmetric four-sheet CPT system (610 mm × 610 mm) with FEA-optimized guard rings and an LCLC compensation network, achieving 92% efficiency at 3.3 kW with ±15 cm lateral or 5–20 cm vertical misalignment tolerance. By harmonizing high-power performance, safety, and adaptability, this design advances CPT toward scalable, real-world EV charging solutions.

1.3. Objectives and Approach

This paper aims to introduce and evaluate two novel symmetric four-sheet pad configurations for CPT systems, designed to enhance the self-capacitance, improve the coupling efficiency, and eliminate the need for oversized or additional passive components, while maintaining compact pad geometry. This study proposes M2-four-sheet parallel and M2-four-sheet stacked formations, both of which differ from traditional designs [9,16] but maintain consistent dimensions (610 mm × 610 mm) and a fixed transfer distance (150 mm). A double-sided LCLC-compensated topology is adopted to support efficient power transfer, and the designs are analyzed using finite-element and circuit-level simulations.

A systematic methodology is followed, including coupler design, performance evaluation, and comparative analysis with existing layouts, to identify performance trade-offs and suitability for practical deployment. The results aim to optimize CPT systems for efficient, scalable, and sustainable wireless EV charging applications.

The remainder of this paper is organized as follows: Section 2 presents the circuit topology of the CPT system. Section 3 describes the circuit model and the formation of the capacitive coupler. The results and discussion are provided in Section 4, and the conclusion is presented in the final section.

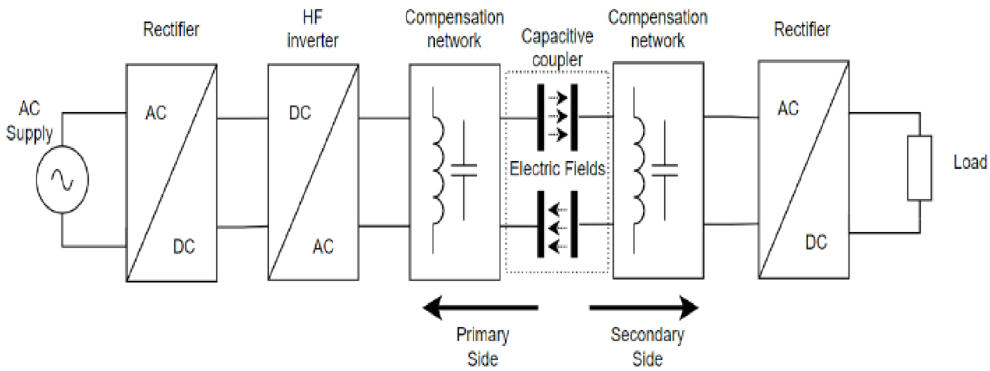

Fig. 1. Typical formation of a CPT system

ISSN 1814-4225 (print)
ISSN 2663-2012 (online)

2. Circuit topology of a CPT system

As previously mentioned, CPT systems rely on two critical components for efficient energy transmission: (1) the design of capacitive couplers and (2) the configuration of compensation networks. These elements influence system performance metrics such as power transfer capability, efficiency, and frequency response [5]. The following sections explore the different types of compensation topologies and the capacitive coupler formations used in CPT systems.

2.1. Compensation Network Topology

In CPT systems, the compensation network plays a critical role in reducing the volt-ampere rating of the power supply, enhancing the power transfer efficiency, and increasing the voltage across the coupling plates. The effective compensation also improves the coupling coefficient and reduces the reactive power, resulting in higher system performance [1, 20].

Compensation networks in CPT systems can generally be categorized into two groups: resonant compensation and non-resonant compensation [5]. An overview of the main compensation topologies used in CPT systems is presented in Fig. 2, which illustrates the classification between resonant and non-resonant schemes and their respective sub-categories. The choice of compensation topology depends on the converter type and the specific performance requirements of the system.

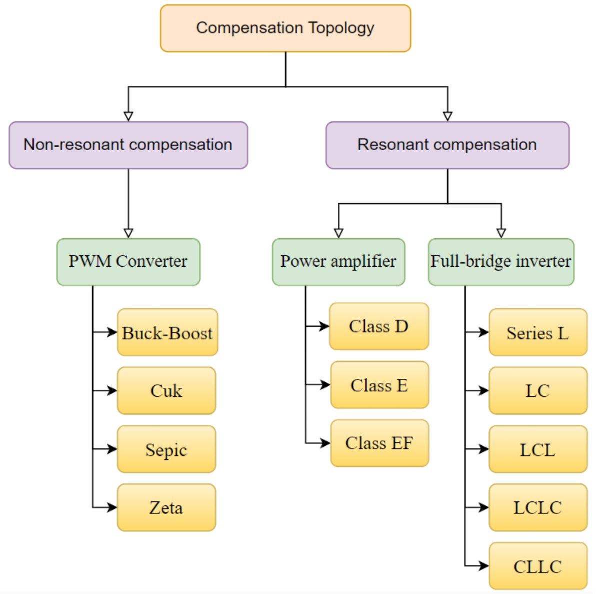

Fig. 2. Compensation Topology Categories

Regarding the excitation methods for CPT systems, PWM-based circuits using a single modulating switch, such as Cuk and Buck-Boost converters, offer robustness against parameter variations. However, they are typically limited to very short transfer distances due to the large coupling capacitances required, which also constrain the system's power scalability. Furthermore, achieving soft-switching conditions is challenging, leading to increased switching losses and elevated EMI issues.

To address the limitations of distance and scalability, power amplifier-based CPT systems were developed. These systems operate at resonant frequencies, allowing higher switching frequencies and reducing the size of reactive components [21]. Although soft switching improves system efficiency, power amplifier-based configurations are highly sensitive to component tolerances, where small parameter variations can significantly affect the resonance stability and overall performance.

As an advancement, full-bridge inverter topology has emerged as a highly efficient method for exciting resonant CPT systems. The proposed full-bridge inverter enables higher power transfer capabilities, better scalability, and more flexible control than single-switch PWM converters. It also facilitates the implementation of advanced LCLC compensation networks [9, 20]. By employing four modulating switches, the full-bridge inverter provides more robust and efficient CPT operation, making it suitable for medium- and high-power applications. In this study, a double-sided LCLC-compensated network driven by a full-bridge inverter was adopted, as shown in Fig. 3. This configuration addresses the challenge of small coupling capacitance by introducing auxiliary capacitors, achieving a unity power factor at both the input and output sides, and providing a load-independent constant current (CC) output with zero-phase-angle (ZPA) operation at the designed resonant frequency [9].

2.2. Capacitive Coupler Formation

The capacitive coupler uses multiple metal sheets to produce electric fields, thereby facilitating power transfer. The formation of the capacitive coupler influences the coupling between each sheet pair, which in turn determines the efficiency of power transmission. This section investigates the key structural aspects of capacitive couplers.

2.2.1. Two-Sheets Formation

To construct a capacitive coupler, it is necessary to use at least two metal sheets, as depicted in Fig. 4. This configuration is occasionally known as a unipolar arrangement.

The mutual capacitance between the two sheets allows the current to flow toward the load. Consequently, a conductive pathway is necessary to facilitate the return of current to the primary side [22, 23]. Unipolar formation offers the benefit of being straightforward and having a high tolerance for significant misalignments [1].

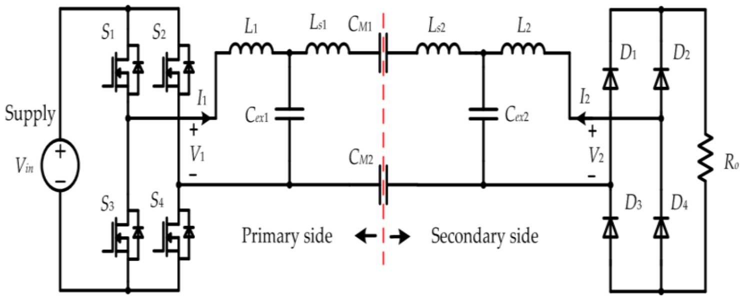

Fig. 3. CPT system based on LCLC Topology [20]

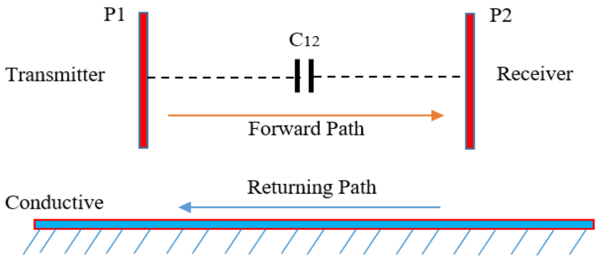

Fig. 4. The design of the two-sheet coupler

2.2.2. Four-Sheet Parallel Formation

The most prevalent method for implementing a capacitive coupler is the four-sheet parallel formation, also known as bipolar formation. This formation consists of two pairs of metal sheets placed in parallel. Fig. 5 shows six capacitances arising from the coupling capacitance between each pair of sheets. The main coupling capacitances are specified as C_{13} and C_{24}. The cross-coupling capacitances were defined as C_{14} and C_{23}. The self-coupling capacitances were defined as C_{12} and C_{34}.

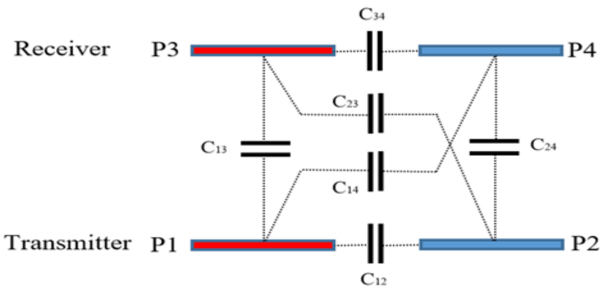

Fig. 5. Four-Sheet Parallel Formation

The modest capacitances C_{12} and C_{34} often limit the self-capacitances in this arrangement. Hence, it is necessary to link extra capacitors to the coupler to augment the overall self-capacitance. Nevertheless, external capacitances typically require more space within the system. In addition, this parallel construction is susceptible to angular misalignment [1, 9].

2.2.3. Four-Sheets Stacked Formation

In order to enhance the self-capacitance and eliminate external capacitances, the primary sheets P_1 and P_2 are positioned in near proximity to one another [1, 24]. Furthermore, the space between the secondary sheets P_3 and P_4 was similarly decreased, as illustrated in Fig. 6. The term "four-sheet stacked formation" is used to describe a configuration in which all sheets are piled together.

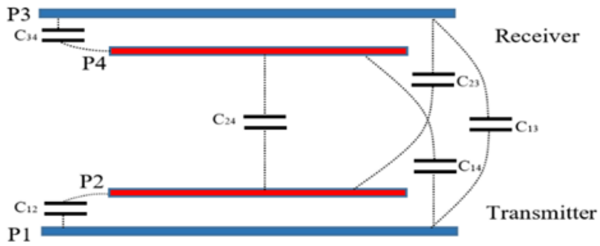

Fig. 6. Four-Sheet Stacked Formation

P_1 and P_3 have a greater size compared to P_2 and P_4 to guarantee the coupling between every pair of sheets. Due to the proximity of the same-side sheets, the capacitances C_{12} and C_{34} can be greatly enhanced. The coupling model of this stacked formation is identical to that of the parallel formation [9]. Due to the positioning of sheets P_2 and P_4 between P_1 and P_3, this stacked coupler provides a significantly more condensed arrangement in comparison to the four-sheet parallel construction. This arrangement reduces the angular misalignment sensitivity. A drawback of this arrangement is the very limited mutual capacitance. Due to the smaller size of the coupler, the cross-coupling capacitances C_{14} and C_{23} were amplified. Equation (3) indicates that the equivalent mutual capacitance C_M is thus diminished. Another crucial consideration in the stacked coupler is the voltage stress that occurs between the sheets on the same side. In particular, in situations involving the transmission of power over long distances, the voltage stress between neighboring sheets is typically extremely high. Hence, it is imperative to apply dependable insulation on the sheet surface [1].

$$C_1 = C_{12} + \frac{(C_{13} + C_{14}) \text{ x } (C_{23} + C_{24})}{C_{13} + C_{14} + C_{23} + C_{24}}, \quad (1)$$

$$C_2 = C_{34} + \frac{(C_{13} + C_{23}) \text{ x } (C_{14} + C_{24})}{C_{13} + C_{14} + C_{23} + C_{24}}, \quad (2)$$

ISSN 1814-4225 (print)
ISSN 2663-2012 (online)

$$C_M = \frac{(C_{24}\,C_{13}) - (C_{14}\,C_{23})}{C_{13} + C_{14} + C_{23} + C_{24}}, \tag{3}$$

$$k_c = \frac{C_M}{\sqrt{C_1 \cdot C_2}}. \tag{4}$$

The coupling coefficient k_c is a key parameter that describes how effectively energy is transferred between capacitive sheets. The value indicates how well the electric field between the primary and secondary sheets is coupled. The efficiency of power transfer is highly dependent on k_c as the following equation [25]:

$$\eta_{max} = \frac{1}{\left[1 + \frac{1}{k_c}\left(\frac{1}{Q_L} + \frac{1}{Q_C}\right)\right]^2}, \tag{5}$$

where Q_L is the quality factor of L_1 and L_2 and Q_C is the quality factor of C_1 and C_2.

Within the scope of this paper, the focus was placed on the structural design of both the four-sheet parallel and four-sheet stacked configurations, as detailed in [9] and [16], respectively. These designs were then compared against two other designs.

3. Circuit Model and Capacitive Coupler Formation

3.1. Capacitive Coupler Design

This study presents the design and analysis of four capacitive coupler models using Maxwell software. The analysis was carried out using four aluminum sheets as part of the coupler construction. A comparative analysis was conducted among the four designs presented. The first model is presented in [9], which contains four metal sheets that have been used to form symmetrical two-coupling capacitors to transfer power, called a "four-sheet parallel formation". The sheet size was set to (610 mm × 610 mm) as shown in Fig. 8.

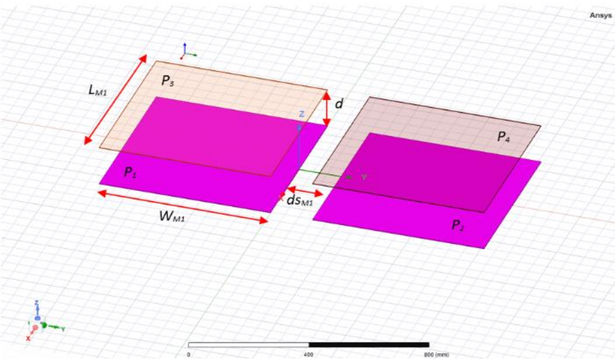

Fig. 8. Three-dimensional view of the four-sheet parallel formation

L_{M1} refers to the length of sheets (P_1, P_2, P_3, P_4), W_{M1} refers to the width of sheets. The distance between P_1–P_3 and P_2–P_4 is dsM1; the distance between P_1–P_2 and P_3–P_4 is d, the air gap separating the secondary and primary sides. The thickness of all sheets was the same.

The second model is presented in [16], which contains four metal sheets. The sheets were symmetrical from the primary to the secondary side. Two sheets are positioned close to one another vertically arranged at both sides to preserve significant coupling capacitance and save space, as depicted in Fig. 9. Therefore, this model is called a "four-sheet stacked formation". P_1 and P_3 are larger than P_2 and P_4. Therefore, the coupling between P_1 and P_3 cannot be eliminated by P_2 and P_4.

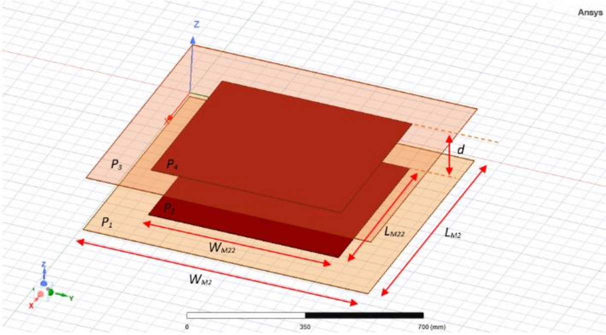

Fig. 9. Three-dimensional view of the four-sheet stacked formation

L_{M2} and W_{M2} refer to the length and width of outer sheets (P_1 and P_3), respectively; L_{M22} and W_{M22} refer to the length and width of inner sheets (P_2 and P_4), respectively; the distance between P_1 and P_2 and between P_3 and P_4 is ds_{M1}, and the distance between P_2 and P_4 is d, which is the air gap between the secondary and primary sides.

The third model has been proposed in this paper; it comprises four parallel sheets similar to the first model, as shown in Fig. 10. The proposed design increases the self-capacitance and maintains high capacitive coupling. This is an important challenge in CPT.

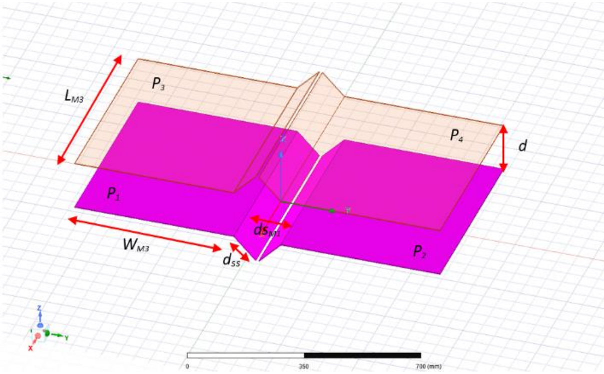

Fig. 10. Three-dimensional view of the M2-four sheet parallel formation

This formation is called the "M2-four-sheet parallel formation". In this design, the width of each sheet is increased from the inner side with a length dss and an angle of 45° to increase the capacitance between P_1 and P_2, P_1 and P_4, P_2, and P_3, and thus increase the efficiency of the system.

The proposed fourth model is similar to the four-sheet stacked formation but has the same sheet size, as shown in Fig. 11. The sheets were positioned to overlap on each side to enhance the self-capacitance and capacitive coupling of the design while maintaining the same sheet area.

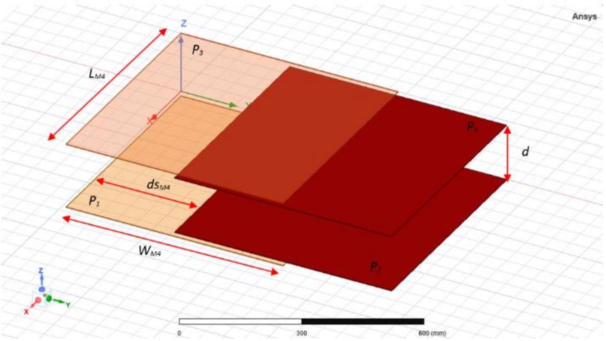

Fig. 11. Three-dimensional view of M2-four sheet stacked formation

ds_{M2} represents the displacement of the P_2 and P_4 sheets from the P_1 and P_3 sheets. In this case, it maintains a high-capacitive coupling between P_1 and P_3. This formation is called "M2-four sheet stacked formation".

The coupling capacitor models for the above four models are shown in Fig. 12.

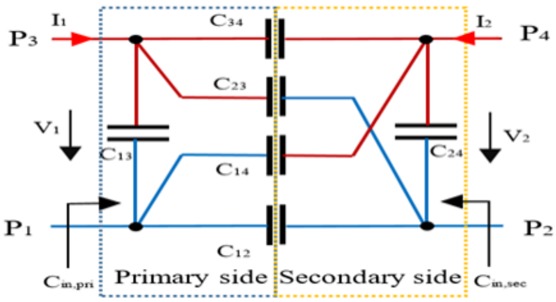

Fig. 12. Model of the coupling capacitors

3.2. Compensation Network Simulation

In this paper, two cases were considered for the compensation network, as shown in Fig. 13. The simulation was conducted using MATLAB software. It was done in two cases: case 1 with parallel formation to add an external capacitance because the coupling capacitance value was small (LCLC topology), and case 2 with the stacked formation to get rid of the external capacitance (LCL topology).

A full-bridge inverter is used on the primary side to generate an excitation Vin for the resonant tank. On the secondary side, a full-bridge rectifier provides DC current to the output battery. At the front end, L_{f1} and C_{f1} function as low-pass filters. In a similar vein, L_{f2} and C_{f2} function as back-end low-pass filters. The fundamental harmonic approximation approach simplifies the system in parallel formation. The circuit parameters were configured to achieve resonance at an identical frequency. The parameter values should satisfy (5), where f_{sw} is the switching frequency [9].

$$\begin{cases} L_{f1} = 1/(\omega_o^2 C_{f1}),\;\; L_{f2} = 1/(\omega_o^2 C_{f2}),\; \omega_o = 2\pi\, f_{sw} \\ L_1 = 1/(\omega_o^2 C_{p1}) + L_{f1},\;\; L_2 = 1/(\omega_o^2 C_{p2}) + L_{f2} \\ C_{p1} = C_{ex1} + [(Cs \times C_{ex2})/(Cs + C_{ex2})] \\ C_{p2} = C_{ex2} + [(Cs \times C_{ex1})/(Cs + C_{ex1})] \\ Cs = C_{13} \times C_{24} / (C_{13} + C_{24}) \end{cases} \tag{6}$$

4. Results and Discussion

4.1. Capacitive Coupler Analysis

The capacitive coupler configurations were analyzed using ANSYS Maxwell software. Each of the four proposed designs generates six mutual capacitances between adjacent sheet pairs, as illustrated in Fig. 12. The geometric parameters of each coupler design are summarized in Table 1.

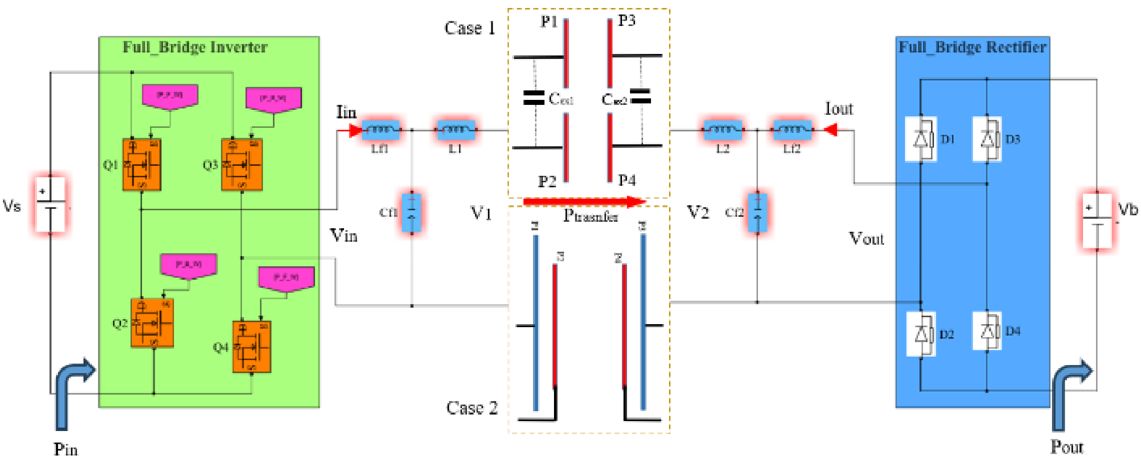

Fig. 13. CPT system

ISSN 1814-4225 (print)
ISSN 2663-2012 (online)

Table 1
Geometric parameters of the coupler formations

Parameter (mm)	Four sheet parallel formation	Four sheet stacked formation	M2-Four sheet parallel formation	M2-four sheet stacked formation
	Value	Value	Value	Value
L_{M1}	610	-----	-----	-----
W_{M1}	610	-----	-----	-----
ds_{M1}	150	-----	150	-----
L_{M2}	-----	914	-----	-----
W_{M2}	-----	914	-----	-----
L_{M22}	-----	610	-----	-----
W_{M22}	-----	610	-----	-----
L_{M3}	-----	-----	610	-----
W_{M3}	-----	-----	510	-----
dss	-----	-----	100	-----
L_{M4}	-----	-----	-----	610
W_{M4}	-----	-----	-----	610
ds_{M4}	-----	-----	-----	305

Coupling capacitors between sheets were calculated by ANSYS Maxwell, and the self-capacitances and mutual capacitances depend on equations (1 to 4). Table 2 lists both the simulated and analytically derived equivalent capacitance values for an air gap of 150 mm.

Table 2
Maxwell-Simulated and Equivalent Capacitances at a 150-mm air gap

Parameter	Four sheet parallel formation	Four sheet stacked formation	M2-Four sheet parallel formation	M2-four sheet stacked formation
	Value	Value	Value	Value
C_{12}	8.295 pF	381.89 pF	58.431 pF	204.92 pF
C_{13}	33.306 pF	41.132 pF	29.336 pF	15.497 pF
C_{14}	4.800 pF	4.972 pF	4.950 pF	4.979 pF
C_{23}	4.814 pF	4.748 pF	5.102 pF	5.000 pF
C_{24}	33.509 pF	20.679 pF	29.09 pF	27.298 pF
C_{34}	8.411 pF	385.43 pF	58.655 pF	205.82 pF
C_1	27.403 pF	398.28 pF	75.552 pF	217.45 pF
C_2	27.519 pF	401.89 pF	75.776 pF	218.15 pF
C_M	14.3 pF	11.56 pF	12.1 pF	7.543 pF
K_c	0.52	0.028	0.16	0.034

The M2-four-sheet stacked formation was designed to enhance the self-capacitance components (C_1 and C_2), while the M2-four-sheet parallel formation was optimized to increase the self-capacitance, maintain high mutual capacitance, and minimize the reliance on external capacitors. The simulation results presented in Table 2 indicate that the self-capacitance of the M2-four-sheet parallel formation is approximately 175% greater than that of the conventional four-sheet parallel formation with identical sheet sizes (see Fig. 10). However, this improvement is accompanied by a slight reduction in mutual capacitance – around 15% lower than that observed in the traditional formation. In contrast, the M2-four-sheet stacked formation achieves a 21.4% increase in the coupling coefficient relative to the conventional four-sheet stacked formation, although its self-capacitance is nearly reduced by half. Compared to the traditional four-sheet parallel formation, this stacked formation offers a self-capacitance increase by a factor of eight, thereby eliminating the need for external capacitors (as illustrated in Fig. 11).

Maxwell software is used to simulate capacitors at various distances between P_1-P_3 and P_2-P_4, air gaps, and misalignment conditions. As presented in Fig. 14(a-b), the mutual capacitance increases by 7.6% in the conventional four-sheet parallel formation and by 16% in the M2-four-sheet parallel formation as the air gap (dsM) increases. Both the mutual and self-capacitance values were found to be sensitive to alignment variations and changes in the air gap (see Figs. 14(c–e)).

Fig. 15 shows that the maximum mutual capacitance was achieved when the lengths of sheets P_1 and P_3 matched those of P_2 and P_4(rd=1), as previously outlined in Fig. 11.

A comparative performance evaluation of all four formations under different misalignment conditions are shown in Fig. 16.

Finally, Fig. 17 illustrates the electric-field distribution around the plates for each coupler formation, highlighting the field uniformity and strength under ideal alignment.

These findings demonstrate that the M2-four-sheet stacked formation is particularly well-suited for applications requiring enhanced self-capacitance and simplified hardware design, such as compact or embedded EV charging systems. Conversely, the M2-four-sheet parallel formation is advantageous in scenarios in which maximizing the coupling coefficient is a priority, even at the expense of lower self-capacitance. Both M2 designs outperform traditional layouts in terms of key performance metrics while preserving compactness and geometric symmetry. Overall, the results demonstrate that strategic coupler geometry and layout optimization significantly improve the efficiency, reliability, and scalability of low-power capacitive wireless charging systems.

4.2. Simulation Results

The MATLAB/Simulink environment was used to simulate the CPT system employing a double-sided LCLC compensation network, as shown in Fig. 13. The simulation was based on the four-sheet parallel formation. Using the equivalent capacitance values obtained from FEA (as summarized in Table 2) and the analytical model expressed in equation (5), the required compensation circuit parameters were calculated. These parameters are listed in Table 3. They were designed to maintain symmetry following the geometric configuration of the coupler. To ensure efficient switching, the Zero Voltage Switching (ZVS) technique was considered. Fig. 18 shows the voltage and current waveforms across the power switches at resonance.

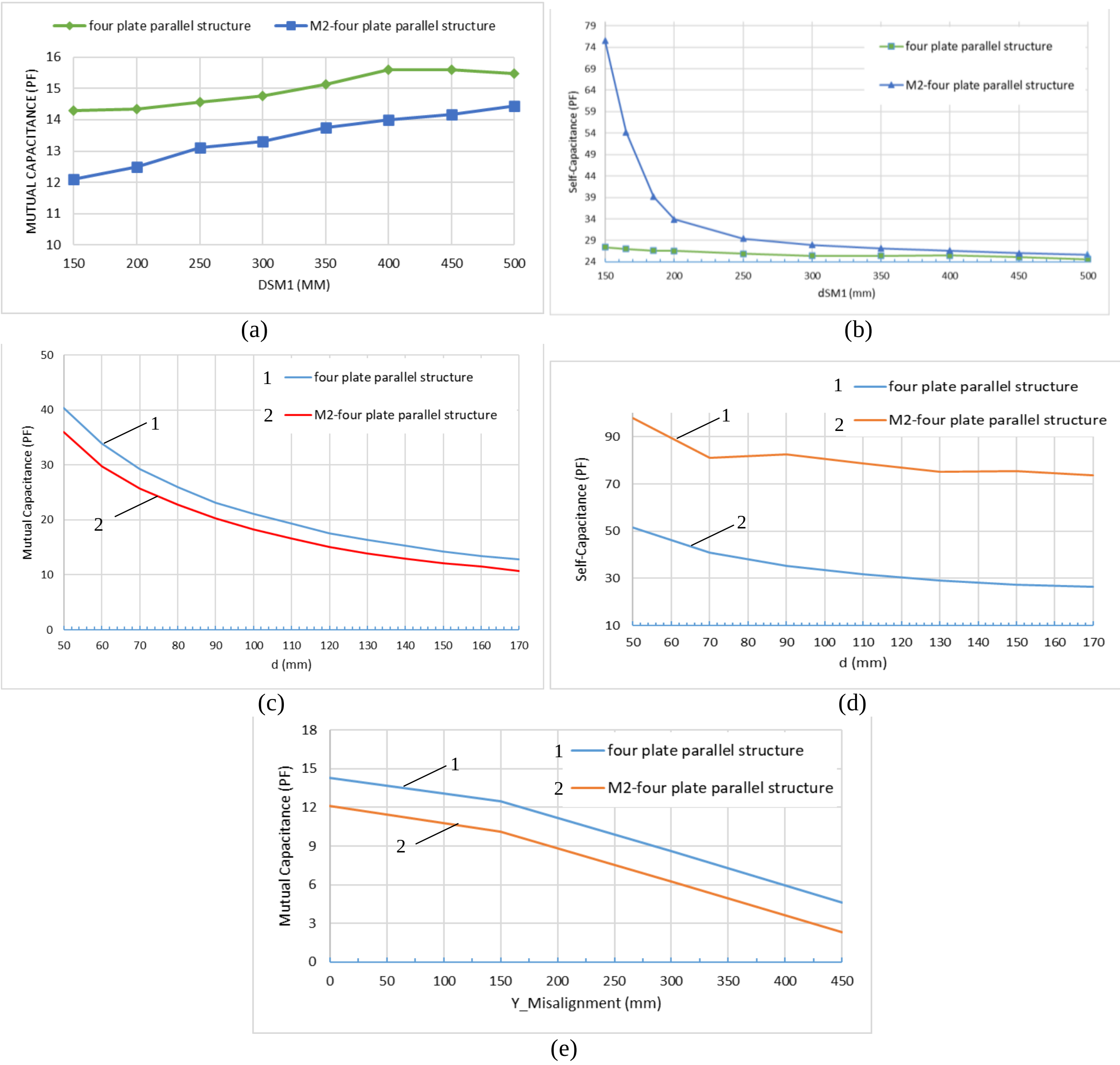

Fig. 14. Capacitance variations with sheet parameters (a) Mutual capacitance at different dS_{M1} (b) Self-capacitance at different dS_{M1} (c) Mutual capacitance at different airgaps (d) Self- capacitance at different airgaps (e) Mutual capacitance at different misalignments

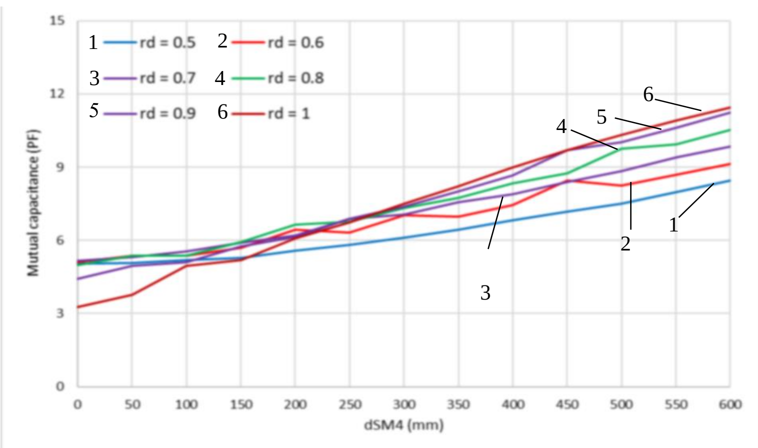

Fig. 15. Mutual capacitance variations with different d_{SM4} values at different r_d for M2- four sheet stacked formation

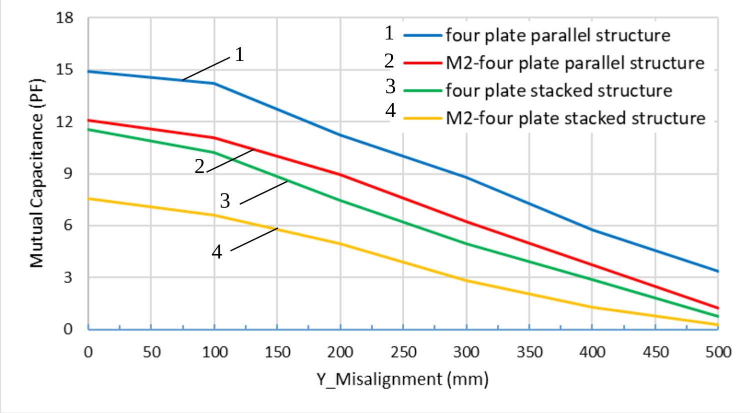

Fig. 16. Mutual capacitance variations with misalignment for four formations

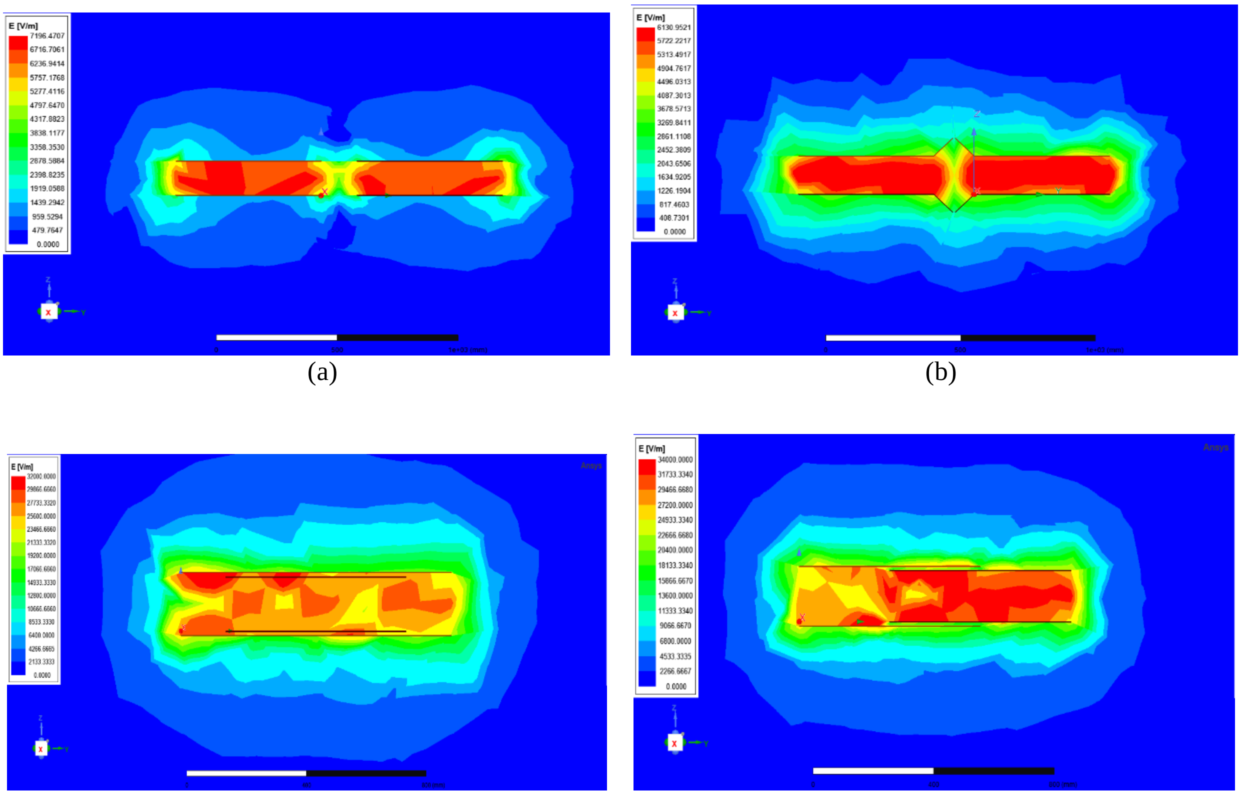

(a) (b)

(c) (d)

Fig. 17. Electric-field strength around the sheets (a) Four-sheet parallel formation (b) M2- four sheet parallel formation (c) Four-sheet stacked formation (d) M2-four-sheet stacked formation

Table 3

System specifications and circuit parameter values (LCLC)

Parameter	Design Value	Parameter	Design Value
Vs	240 V	Vb	260 V
Cf1	2 nF	Cf2	2 nF
Lf1	12.7 μH	Lf2	12.7 μH
Cex1	95 pF	Cex2	95 pF
L1	245 μH	L2	245 μH
fsw	1 MHz	C13 = C24	33.306 pF

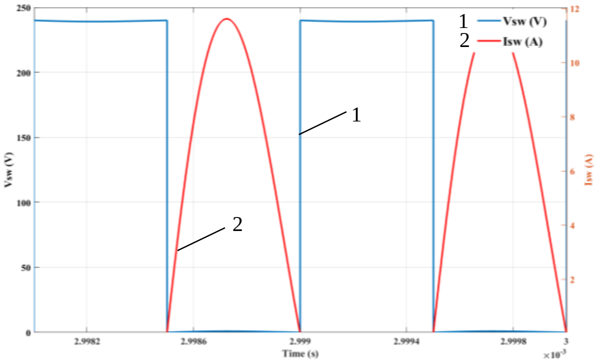

Fig. 18. VSI Transistor Switching Voltage (V_{CE}) and Current (Ic)

Fig. 19 displays the simulated waveforms of the CPT system. The input voltage (Vin) leads to the output voltage (Vout) by 90° and is nearly in phase with the input current (Iin). The output power was 1.58 kW with a DC-DC efficiency of 90.78%, as listed in Table 4. Minor power losses were observed across the inverter, rectifier, and compensation networks.

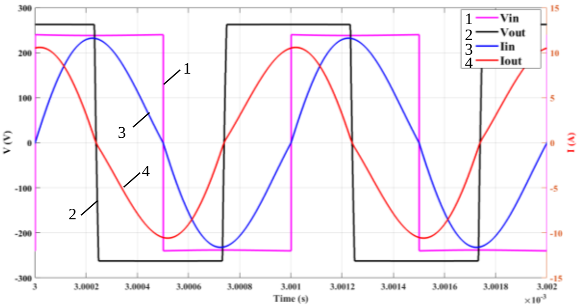

Fig. 19. Simulated input and output voltage and current waveforms for a four-sheet parallel formation

Table 4

Simulation Result

Parameter	Design Value
Pout	1.58 kW
DC-DC Efficiency	90.78 %
VP1-P3 (RMS)	2.6 kV
VP2-P4 (RMS)	2.6 kV
VP1-P2 (RMS)	6.1 kV
VP3-P4 (RMS)	6.1 kV

For the M2-four-sheet stacked formation, the LCL compensation circuit was simulated without requiring an external capacitor. The equivalent capacitor network was simplified to a π-model, as shown in Fig. 20. Using FEA and the analytical expression (6), the design parameters were calculated, as presented in Table 5.

$$\begin{cases} Cin_{,pri} = C_1 - CM + [CM(\,C2\ - C_M\,)/(\,C2\,)] \\ Cin_{,sec} = C_2 - CM + [CM(\,C1\ - C_M\,)/(\,C1\,)] \\ L_1 = 1/(\omega_o^2\, Cin_{,pri}) + L_{f1},\ \ L_2 = 1/(\omega_o^2\, Cin_{,sec}) + L_{f2} \end{cases} \tag{7}$$

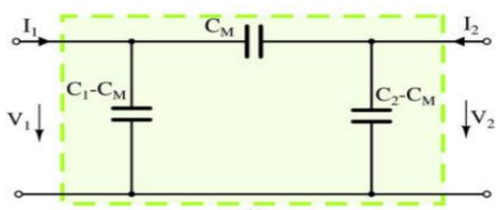

Fig. 20. π model for a four-sheet stacked formation

The simulated waveforms of the CPT system are shown in Fig. 21. The output power of the system using the M2-four-sheet stacked formation was found to be 1.51 kW with a DC-DC efficiency of 90.5% at a 150-mm air gap and perfect alignment. Thus, this model provides the same output power and efficiency without the need for external capacitors and with the same sheet size. Fig. 21 and Fig. 22 illustrate the voltage and current waveforms, as well as the instantaneous and average power profiles of the input source and load for the M2-four-sheet stacked structure.

Table 5

System specifications and circuit parameter values (LCL)

Parameter	Design Value	Parameter	Design Value
Vs	250 V	Vb	260 V
Cf1	5.69 nF	Cf2	5.69 nF
Lf1	4.456 μH	Lf2	4.456 μH
C_M	7.543 pF	fsw	1 MHz
L1	120.83 μH	L2	120.83 μH
C_1-C_M = =C_2-C_M	210.46 pF	$C_1 = C_2$	218 pF

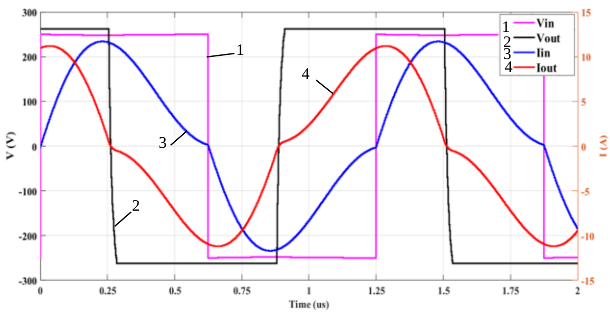

Fig. 21. Simulated input and output voltage and current waveforms for the M2-four sheets stacked formation.

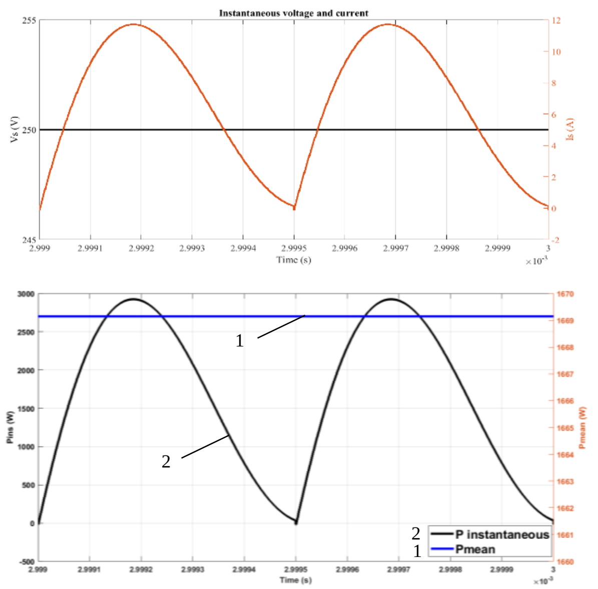

Fig. 22. Input voltage, current, and power for the M2-four sheets stacked formation

ISSN 1814-4225 (print)
ISSN 2663-2012 (online)

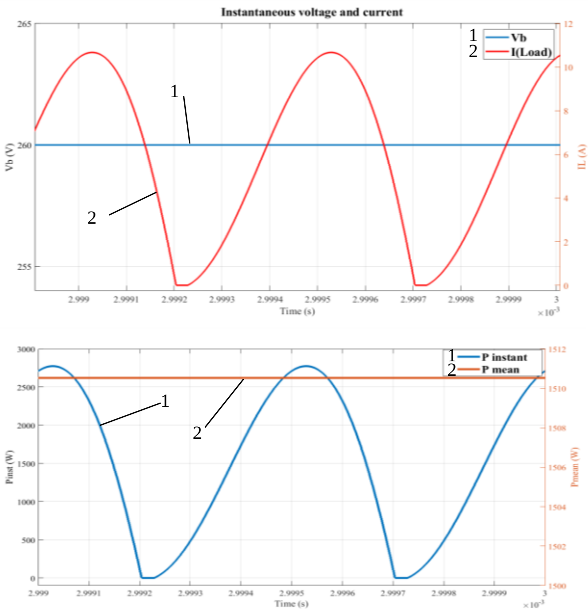

Fig. 23. Output voltage, current, and power for the M2-four sheets stacked formation

4.3. Discussion

The proposed CPT system exhibits significant performance improvement by using symmetric four-sheet pad configurations. The M2-four-sheet parallel formation exhibits high self-capacitance with minimal variation in the coupling capacitance, thereby enhancing the power transfer efficiency compared to the traditional layout. In contrast, the M2-four-sheet stacked formation improved the coupling capacitance but nearly half the self-capacitance relative to the traditional configuration. In addition, it offers better vertical misalignment tolerance than conventional stacked designs.

Quantitatively, the M2-parallel configuration achieved a 175% increase in self-capacitance compared to the traditional parallel layout and a DC-DC efficiency exceeding 90.5%. Meanwhile, the M2-stacked formation provides a 21.4% improvement in the coupling coefficient compared with conventional stacked designs, validating the effectiveness of the proposed modifications in achieving the targeted performance metrics outlined in the study's aim.

From a comparative perspective, the stacked formation achieves higher self-capacitance than the parallel configuration, effectively eliminating the need for external capacitors. Meanwhile, the parallel formation, despite its enhanced coupling efficiency, may still require external capacitors to maintain the system stability under varying load conditions. These findings suggest that the selection of pad configuration should be based on application-specific requirements.

For instance, the parallel configuration is better suited for environments in which high coupling efficiency is critical, provided that external capacitors are added to compensate for low self-capacitance. Conversely, the stacked configuration is preferable for dynamic applications requiring greater resilience to vertical misalignment, compact size, and simpler system architecture without external capacitors.

However, several limitations should be acknowledged. Although the stacked configuration offers improved tolerance to vertical misalignment compared to conventional designs, the system's overall performance remains sensitive to lateral misalignments, which could impact its practicality in dynamic or mobile environments. Moreover, this analysis relies on idealized simulation models and does not fully account for real-world factors such as parasitic capacitances, temperature-induced variations, and material imperfections.

Despite these limitations, the results provide a strong foundation for practical deployment. The proposed system provides a compact, efficient, and scalable solution for low-power wireless EV charging applications. Future work will focus on experimental validation, investigating losses under actual operating conditions, and optimizing the material properties and coupler geometries to further enhance the performance and misalignment resilience.

5. Conclusions

This study presents two novel capacitive coupler designs M2-four-sheet parallel, and M2-four-sheet stacked configurations to overcome the significant limitations of traditional four-plate CPT systems. The M2 four-sheet parallel configuration, combined with an LCLC compensation network, attains 175% greater self-capacitance than conventional parallel designs, thereby obviating the necessity for external capacitors and diminishing the coupling capacitance by 15%. The M2 four-sheet stacked configuration employing an LCL compensation topology enhances the coupling coefficient by 21.4% while maintaining symmetrical sheet dimensions that eliminate the complications associated with oversized outer plates, albeit with some sacrifice in the self-capacitance value compared to the traditional stacked design. Both designs markedly improve system efficiency: when applied in a 1.5 kW CPT system with a 150 mm air gap, they attain over 90.5% DC-DC efficiency, illustrating their suitability for high-performance applications such as EV charging and industrial robotics, where compact geometry and alignment tolerance are essential.

Future research development: Future research will focus on experimental validation of the proposed designs under dynamic operating conditions, including variable loads and lateral misalignment. Further optimization of adaptive compensation networks to maintain resonance across coupling variations, as well as scaling the system for higher power levels (e.g., >10 kW) while addressing electromagnetic interference challenges, will also be explored. These efforts aim to bridge the gap between simulation-based advancements and real-world CPT deployment.

Contributions of authors: Conceptualization, methodology, research problem formulation, and motivation of the research direction. – **Yasir M.Y. Ameen;** design, analysis, development of model, software, verification – **Marwan H. Mohammed;** analysis of results, visualization – **Basil M. Saied.**

Conflict of Interest

The authors declare that they have no conflict of interest in relation to this research, whether financial, personal, authorship or otherwise, that could affect the research and its results presented in this paper.

Financing

This study was conducted without financial support.

Data Availability

The work has associated data in the data repository.

Use of Artificial Intelligence

The authors confirm that they did not use artificial intelligence methods while creating the presented work.

Acknowledgments

We thank the University of Mosul for its technical support and valuable advice throughout the research phases.

All the authors have read and agreed to the published version of this manuscript.

References

1. Lu, F., Zhang, H., & Mi, C. A review on the recent development of capacitive wireless power transfer technology. In Energies *MDPI AG*, 2017, vol. 10, no, 11, pp. 1-30. DOI: 10.3390/en10111752.

2. Wang, F., Yang, Q., Zhang, X., Chen, T., & Li, G. Enhancing Misalignment Tolerance in Hybrid Wireless Power Transfer System with Integrated Coupler via Frequency Tuning. *IEEE Transactions on Power Electronics*, 2024, vol. 39, no. 9, pp. 11885-11899. DOI: 10.1109/TPEL.2024.3416172.

3. Mohammed, M. H., Ameen Y. M. Y., & Mohamed, A. A. S. Dish-Shape Magnetic Flux Concentrator for Inductive Power Transfer Systems. *Int. J. Elec. & Elecn. Eng. & Telecom*, 2020, vol. 9, no. 6, pp. 455–461. DOI: 10.18178/ijeetc.9.6.455-461.

4. Ismael, M. T., Ameen, Y. M. Y., & Mohammed, K. K. Design considerations to improve the coupling-coefficient for the DD charging pad in wireless power transfer applications. *AIP Conference Proceeding*, 2023, vol. 2787, no. 1. AIP Publishing. DOI: 10.1063/5.0148712.

5. Wang, Z., Zhang, Y., He, X., Luo, B., & Mai, R. Research and Application of Capacitive Power Transfer System: A Review. *Electronics (Switzerland) MDPI*, 2022, vol. 11, no. 7. DOI: 10.3390/electronics11071158.

6. Li, H., Liu, Y., & Fu, M. Circular Capacitive Coupler with Multilayer Interleaving for Stable Output. *IEEE Transactions on Microwave Theory and Techniques*, 2023, vol. 71, no. 2, pp. 719-726. DOI: 10.1109/TMTT.2022.3201249.

7. Mohammed, M. H., Ameen, Y. M. Y., & Mohamed, A. A. S. A Combined Rectangular/Circular Power Pad for Electric Vehicles Wireless Charging. *2021 IEEE Green Technologies Conference (GreenTech)*, Denver, CO, USA, 2021, pp. 195-200. DOI: 10.1109/GreenTech48523.2021.00041.

8. Abramov, E., & Peretz, M. M. Modeling and Analysis of Capacitive Wireless Power Transfer Systems: A Network Approach. *2018 IEEE International Power Electronics and Application Conference and Exposition (PEAC)*, Shenzhen, China, 2018, pp. 1-6. DOI: 10.1109/PEAC.2018.8590399.

9. Lu, F., Zhang, H., Hofmann, H., & Mi, C. A Double-Sided LCLC-Compensated Capacitive Power Transfer System for Electric Vehicle Charging. *IEEE Transactions on Power Electronics*, 2015, vol. 30, no.11, pp. 6011-6014. DOI: 10.1109/TPEL.2015.2446891.

10. Zhang, J., Yao, S., Pan, L., Liu, Y., & Zhu, C. A Review of Capacitive Power Transfer Technology for Electric Vehicle Applications. *Electronics*, 2023, no. 16, article no. 3534. DOI: 10.3390/ electronics12163534.

11. Marcrum, T., Williams, J.-C., C. S., Johnson, C. S., Pearce, M., Pope, C., Van Neste, C. W., Vaughan, C., & Boyd, D. Quasi-Wireless Capacitive Power Transfer for Wire-Free Robotic Joints. *Energies*, 2024, vol. 17, no. 12, article no. 2858. DOI: 10.3390/en17122858.

12. Shmilovitz, D., Abramovitz, A., & Reichman, I. Quasi-Resonant LED Driver with Capacitive Isolation and High PF. *IEEE Journal of Emerging and Selected Topics in Power Electronics*, 2015, vol. 3, no. 3, pp. 633-641. DOI: 10.1109/JESTPE.2015.2419882.

13. Hu, A. P., Liu, C., & Li., H. L. A Novel Contactless Battery Charging System for Soccer Playing Robot. *2008 15th International Conference on Mechatronics and Machine Vision in Practice, Auckland, New Zealand*, 2008, pp. 646-650. DOI: 10.1109/MMVIP. 2008.4749606.

14. Ludois, D. C., Erickson, M. J., & Reed, J. K. Aerodynamic Fluid Bearings for Translational and Rotating Capacitors in Noncontact Capacitive Power Transfer Systems. *IEEE Transactions on Industry Applications*, 2014, vol. 50, no. 2, pp. 1025-1033. DOI: 10.1109/ TIA.2013.2273484.

ISSN 1814-4225 (print)
ISSN 2663-2012 (online)

15. Li, S., Liu, Z., Zhao, H., Zhu, L., Shuai, C.& Chen, Z. Wireless Power Transfer by Electric Field Resonance and Its Application in Dynamic Charging," *IEEE Transactions on Industrial Electronics*, 2016, vol. 63, no. 10, pp. 6602-6612. DOI: 10.1109/TIE.2016. 2577625.

16. Zhang, H., Lu, F., Hofmann, H., Liu, W., & Mi, C. C. A Four-Sheet Compact Capacitive Coupler Design and LCL-Compensated Topology for Capacitive Power Transfer in Electric Vehicle Charging Application. *IEEE Transactions on Power Electronics*, 2016, vol. 31, no. 12, pp. 8541-8551. DOI: 10.1109/TPEL.2016.2520963.

17. Rong, E., Sun, P., Qiao, K., Zhang, X., Yang, G., & Wu, X. Six-Plate and Hybrid-Dielectric Capacitive Coupler for Underwater Wireless Power Transfer. *IEEE Transactions on Power Electronics*, 2024, vol. 39, no. 2, pp.2867-2881. DOI: 10.1109/TPEL.2023.3334888.

18. Chen, T., Cheng, C., Zhang, X., Li, G., Guo, Y. & Mi, C. C. A Double-Sided LCL-Compensated Network for the Strongly Coupled CPT System with Minimum Plate Voltage Stresses. *IEEE Journal of Emerging and Selected Topics in Power Electronics*, 2024, vol. 12, no. 4, pp. 4275-4287. DOI: 10.1109/JESTPE. 2024.3400874.

19. Estevez-Encarnacion, E. S, Hernandez-Gonzalez, L., Ramirez Hernandez, J., Juarez-Sandoval, O. U., Guevara-Lopez, P., & Avalos Arzate, G. Design of Stabilizing Network for Capacitive Power Transfer Transmitter Operating at Maximum Power Transfer Limiting the Voltage Gain in Resonant Capacitors. *Electronics*, 2024, vol. 13, no. 19, article no. 3859. DOI: 10.3390/electronics13193859.

20. Li, L., Wang, Z., Gao, F., Wang, S., & Deng, J. A family of compensation topologies for capacitive power transfer converters for wireless electric vehicle charger. *Applied Energy*, 2020, vol. 260, DOI: 10.1016/j.apenergy.2019.114156.

21. Huang, L., Hu, A. P., & Swain, A. A resonant compensation method for improving the performance of capacitively coupled power transfer system. *2014 IEEE Energy Conversion Congress and Exposition (ECCE)*, Pittsburgh, PA, USA, 2014, pp. 870-875. DOI: 10.1109/ECCE.2014.6953489.

22. Liang, J., Wu, D., & Yu, J., A design method of compensation circuit for high-power dynamic capacitive power transfer system considering coupler voltage distribution for railway applications. *Electronics (Switzerland)*, 2021, vol. 10, no. 2, pp. 1–17. DOI: 10.3390/electronics 10020153.

23. Lu, F., Zhang, H., & Mi, C. A Two-Plate Capacitive Wireless Power Transfer System for Electric Vehicle Charging Applications. *IEEE Transactions on Power Electronics*, 2018, vol. 33, no. 2, pp. 964-969. DOI: 10.1109/TPEL.2017. 2735365.

24. Komaru, T., & Akita, H. Positional characteristics of capacitive power transfer as a resonance coupling system. *2013 IEEE Wireless Power Transfer (WPT)*, Perugia, Italy, 2013, pp. 218-221, DOI: 10.1109/WPT.2013.6556922.

25. Wu, Y., Chen, Q., Ren, X., & Zhang, Z. Efficiency Optimization Based Parameter Design Method for the Capacitive Power Transfer System, *IEEE Transactions on Power Electronics*, 2021, vol. 36, no. 8, pp. 8774-8785. DOI: 10.1109/TPEL.2021.3049474.

Received 1.07.2024, Accepted 20.05.2025

ЕФЕКТИВНЕ ПРОЄКТУВАННЯ СИСТЕМИ БЕЗДРОТОВОГО ЗАРЯДЖАННЯ НА ОСНОВІ ЄМНІСНОГО З’ЄДНАННЯ ДЛЯ МАЛОПОТУЖНИХ ЗАСТОСУВАНЬ

Ясір М.Й. Ateen, Марван Х. Мохаммед, Базіл Мохаммед Саїд

Предметом статті є проєктування та аналіз зарядних панелей на основі ємнісного з’єднання для систем бездротової передачі енергії (WPT), що використовуються в системах заряджання електричних транспортних засобів (EV). **Основна мета цього дослідження** – підвищити ефективність та загальну продуктивність систем заряджання EV, що базуються на ємнісній передачі енергії (CPT), шляхом покращення власної ємності, збільшення коефіцієнта зчеплення та мінімізації залежності від надмірних або допоміжних пасивних компонентів при збереженні компактної геометрії панелей. Для досягнення цієї мети запропоновано та оцінено дві нові конфігурації чотиришарових панелей: M2 – паралельна чотиришарова форма, де чотири алюмінієві пластини розташовані горизонтально, та M2 – мікроскладена чотиришарова форма, де пластини вирівняні вертикально. Їх продуктивність систематично порівнюється з традиційними чотиришаровими конфігураціями для підтвердження запропонованих покращень. Обидві запропоновані конфігурації мають однакові розміри панелей (610 мм × 610 мм) на первинній та вторинній стороні, щоб забезпечити ефективне з’єднання та високу самочастотність. Використані **методи** включають застосування компенсаційних топологій LCLC та LCL для створення резонансу з ємнісним з’єднувачем і подачі високої напруги на зарядні панелі. Метод скінченних елементів (FEM) використовується для моделювання ємності зв’язку та оптимізації геометрії з’єднувача, а програмне забезпечення MATLAB – для моделювання всієї системи WPT. **Результати** показують, що M2-паралельне чотирипластинне формування забезпечує значно вищу самочастотність порівняно з традиційною схемою при незначній зміні ємності зв'язку. М2-стекове формування демонструє ще вищу самочастотність, ніж паралельне, і покращує загальну ефективність системи без збільшення розміру панелей. Було спроєктовано систему СРТ потужністю 1,5 кВт із чотирма алюмінієвими пластинами та повітряним зазором 150 мм, яка досягла ефективності DC-DC понад 90,5%. **Висновки.** Конфігурація М2-паралельне формування демонструє збільшення самочастотності на 175% порівняно з традиційною схемою, що зменшує залежність від зовнішніх конденсаторів. У свою чергу, М2-стекове формування покращує коефіцієнт зв'язку на 21,4%, хоча й зменшує самочастотність майже вдвічі. Обидві конфігурації суттєво покращують ефективність і продуктивність систем бездротового заряджання електромобілів. У цьому дослідженні представлено нову симетричну конструкцію з чотирьох пластин, яка значно покращує власну ємність і коефіцієнт зв'язку, що дозволяє зменшити залежність від зовнішніх конденсаторів при збереженні компактних розмірів і високої ефективності передавання енергії.

Ключові слова: Бездротова передача потужності (WPT); ємнісна передача потужності; зарядка електромобіля; компенсація LCLC; компенсація LCL; формування чотирьох листів; конструкція ємнісного з'єднувача.

Ясір М. Й. Ameen – отримав ступінь бакалавра, магістра та доктора філософії з інженерії електроенергії та електричних машин в Університеті Мосула в 1997, 2000 і 2008 роках відповідно. Є членом Іракської спілки інженерів (IEU). Викладач на кафедрі електротехніки. Наукові інтереси включають силову електроніку, електричні машини та їхні приводи. Афіліація: кафедра електротехніки, інженерний коледж, Університет Мосула, Мосул, 41001, Ірак.

Марван Х. Мохаммед – отримав ступінь бакалавра наук. (2014) та магістра (2020) з електротехніки на факультеті електроенергетики та машин Мосульського університету, Ірак. Викладач кафедри електротехніки. Дослідницькі інтереси включають силову електроніку, проектування та аналіз бездротових систем передачі енергії. Афіліація: кафедра електротехніки Інженерного коледжу Мосульського університету, Мосул, 41001, Ірак.

Базіл Мохаммед Саїд – ступінь доктора філософії Батського університету, Велика Британія, ступінь магістра наук Бредфордського університету, Велика Британія, та ступінь бакалавра наук Мосульського університету, Ірак. Професор Саїд раніше був професором кафедри електротехніки Мосульського університету. Основні наукові інтереси – силова електроніка, приводи, якість електроенергії та електричні машини. Афіліація: кафедра електротехніки Інженерного коледжу Мосульського університету, Мосул, 41001, Ірак.

Dr. Yasir M. Y. Ameen – Bachelor, Master, and Ph.D. degree in Power and Electrical Machines Engineering from the University of Mosul in 1997, 2000, and 2008 respectively. He is a member in Iraqi Engineers Union (IEU). Lecturer in Department of Electrical Engineering. His research interests include power electronics, electrical machines and their drives. His affiliation is Department of Electrical Engineering, College of Engineering, University of Mosul, Mosul, 41001, Iraq.
e-mail: yasir_752000@uomosul.edu.iq, ORCID: 0000-0002-2878-8165, Scopus Author ID: 6507454089.

Mr. Marwan H. Mohammed – B.Sc. (2014) and M.Sc. (2020) degrees in Electrical Engineering from the Electrical Power and Machines Department, Mosul University, Iraq. He is a Lecturer in Department of Electrical Engineering. His research interests include power electronics, design and analysis of wireless power transfer systems. His affiliation is Department of Electrical Engineering, College of Engineering, University of Mosul, Mosul, 41001, Iraq.
e-mail: marwan.alibraheem@uomosul.edu.iq, ORCID: 0009-0001-3208-8671, Scopus Author ID: 57221437441.

Prof. Dr. Basil Mohammed Saied – PhD degree from the university of Bath, UK, MSc degree from university of Bradford, UK, and BSc from the university of Mosul, Iraq. Prof. Saied was formerly professor at Electrical engineering department at University of Mosul. His major research interest in power electronics, drives, power quality and electrical machines. His affiliation is Department of Electrical Engineering, College of Engineering, University of Mosul, Mosul, 41001, Iraq.
e- mail: basil.al.hashimie@uomosul.edu.iq, ORCID: 0000-0002-9891-1851, Scopus Author ID: 6506161609.